LASER INTERFEROMETER GRAVITATIONAL WAVE OBSERVATORY
-LIGO-
CALIFORNIA INSTITUTE OF TECHNOLOGY
MASSACHUSETTS INSTITUTE OF TECHNOLOGY

Technical Note **LIGO-T990100- 00- D** 5/28/99

Simulation of Input Optics with LIGO End-to-End Model

S. Klimenko, G. Mitselmakher and M. Rakhmanov

California Institute of Technology
LIGO Project - MS 18-34
Pasadena CA 91125
Phone (626) 395-2129
Fax (626) 304-9834
E-mail: info@ligo.caltech.edu

Massachusetts Institute of Technology
LIGO Project - MS NW17-161
Cambridge, MA 02139
Phone (617) 253-4824
Fax (617) 253-4824
E-mail: info@ligo.mit.edu

WWW: http://www.ligo.caltech.edu/

file /tex/ionote/T990100.ps

Contents

1 Purpose

This note presents the description of the LIGO Input Optics simulation program which is implemented in the frame of the End-to-End model.

2 Scope

The IO simulation program is built using the End-to-End simulation package [1, 2] specifically developed for the time-domain simulation of the LIGO interferometers. The End-to-End package provides a tool-box that includes primitive, object-oriented modules to describe the LIGO detector components [3]. The primitive modules like field generator, mirrors or digital filters, can be combined together to build more complicated modules that represent different parts of the optical and control systems of the detector. The capabilities of the model include fast cavity simulation (summation modules), simulation of the optical elements dynamic, propagation of a multi-mode Gaussian beam.

Using the End-to-End simulation package we have developed a simulation module for the Input Optics system. It includes all necessary optical elements and the IO control system. Along with the prestabilazed laser (PSL) and Core Optics modules, this module is used to build the Hanford 2K interferometer simulation program.

We also have developed and tested a set of the End-to-End primitive modules including different types of mirrors, thick lens and mode-cleaner summation cavity. This modules were developed using a fast numerical Field Composition-Decomposition (FCD) method [4]. This primitives were extremely useful for development of the IO simulation module and for testing and validation of the standard End-to-End modules.

3 IO simulation layout

Developing the IO simulation module we followed the IO final design document [5]. The Input Optics system consists of the following units:

- RF modulation
- Steering and conditioning optics
- Mode Cleaner and controls
- IFO mode matching
- IFO signal extraction for ASC
- Signal extraction for PSL intensity control

The main beam (psl_beam input port) enters the Input Optics at (x=60.5 in, y=12.5 in) in the PSL optical table local coordinate system. The beam waist is located in this point and the spot size is 0.5 mm.

Figure 1: Internal view of the main IO module.

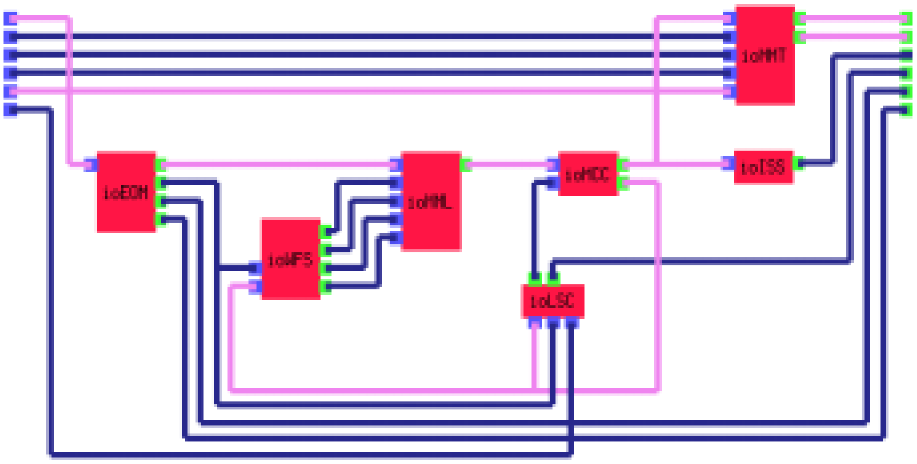

The IO simulation layout is shown in Figure 1, which represents the internal view of the main IO module (configuration file ioo.box). The input and output ports of the main IO module are show in Table 1.

Building the IO module, we tried to follow the physical hardware implementation for each subsystem. The RF modulation unit is described in the ioEOM submodule. The conditioning optics (mode-matching lens telescope) and steering mirrors are placed into the ioMML submodule. The ioMCC submodule contains the mode-cleaner triangular cavity. The main IFO mode-matching is provided by the ioMMT submodule. This submodule also extracts the reflected IFO signal for the ASC control loop. The ioISS submodule generates the PSL intensity stabilization signal. The IO control loops are described by the ioLSC and ioWFS submodules.

All this submodules actually are compound modules that contain the low level submodules and primitive modules. In the following sections we give a detail description of the IO submodules.

4 Model of IO optical elements

Implementing the IO optical system we described only the optical elements that are critical for the IO operation. For example, we didn't describe the flat turning mirrors that are used to keep the beam inside the IO enclosure.

4.1 EOM

The internal view of the ioEOM module is shown in Figure 2. It has one input and four output ports (Table 2).

The k_mcl, k_non, k_res modulation frequencies are generated inside the ioEOM module and distributed to demodulate the control signals. The $L1\_L2$ block is a primitive telescope module [3] that describes two lenses on the input of the IO system.

Table 1: **The IO main module input/output ports.**

input	type	description
psl_beam	field	main PSL beam
mmt3_yaw	real	control yaw signal for MMT3 mirror
mmt3_pitch	real	control pitch signal for MMT3 mirror
mmt3_lsc	real	control z-position signal for MMT3 mirror
ifo_reflected	field	IFO reflected light
offset	real	offset signal for the IO control loop

output	type	description
io_beam	field	main IO beam
FI_reflected	field	IFO reflected light extracted from Faraday isolator
PSL_ISS	real	PSL intensity stabilization signal
WBS	real	Wide Band Servo signal for PSL
k_non-resonant	real	IFO non-resonant sideband modulation frequency
k_resonant	real	IFO resonant sideband modulation frequency

Figure 2: Internal view of the beam modulation module.

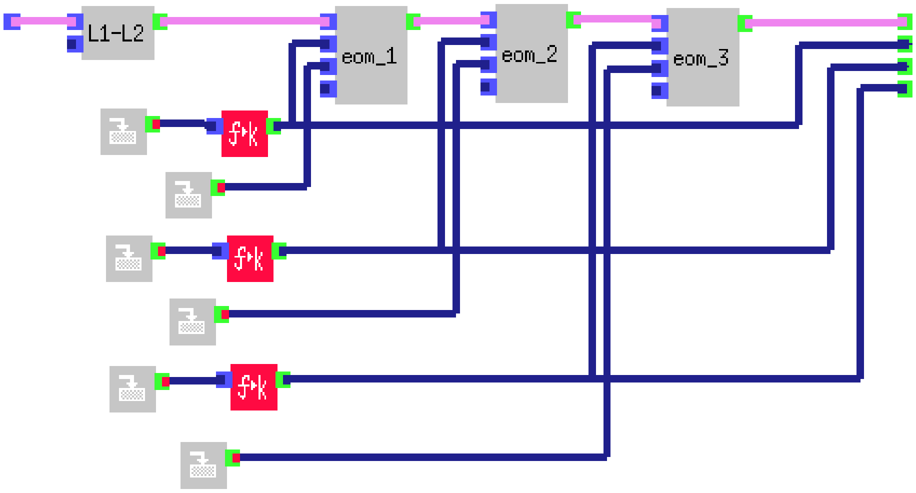

Table 2: **The ioEOM module input/output ports.**

input	type	description
beam	field	input beam
output	type	description
out	field	output beam
k_mcl	real	MC lock sideband modulation frequency
k_non	real	IFO nonresonant sideband modulation frequency
k_res	real	IFO resonant sideband modulation frequency

Figure 3: Pockel cell module.

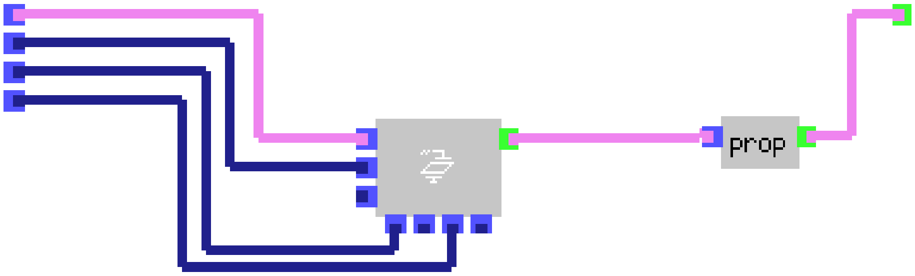

The Pockel cells are implemented (EOM_1, EOM_2, EOM_3) using one base module (eom.box) that contains the $sideband\_gen$ and $propagator$ primitive modules (Figure 3). The EOM parameters (modulation frequency and depth) are specified using the $data\_in$ primitive modules. The parameter settings we used to describe the Hanford 2K interferometer RF modulation are shown in Table.3.

4.2 Mode-Matching lens telescope and steering mirrors

The internal view of the ioMML module is shown in Figure. 4 and input/output ports are listed in Table. 4. The ioMML module contains the mode-matching telescope (MML) and two steering mirrors (PM2, TM5) with active control to optimize the mode-matching into the Mode Cleaner cavity. The $tm5SC$ and $pm2SC$ modules describe the steering mirror Suspension Controllers that receive the control signals from the WFS control loop. Table. 5 shows the parameter settings we used in the simulation.

Table 3: **The ioEOM primitive module's parameter settings.**

name	primitive	parameter	settings	description
L1_L2	telescope	length	1.24	total telescope length
		lensinfo	(0.,0.6373),(1.065,0.6373)	lens's parameters
f_EOM1	data-in	real	26.717e6	EOM-1 modulation frequency
g_EOM1	data-in	real	0.1	EOM-1 modulation depth
f_EOM2	data-in	real	68.800e6	EOM-2 modulation frequency
g_EOM2	data-in	real	0.055	EOM-2 modulation depth
f_EOM3	data-in	real	29.486e6	EOM-3 modulation frequency
g_EOM3	data-in	real	0.47	EOM-3 modulation depth
prop	propagator	have-delay	no	non-delay propagator
		length	0.102	distance between Pockel cells

Figure 4: Mode-Matching lens telescope and steering mirrors (ioMML module).

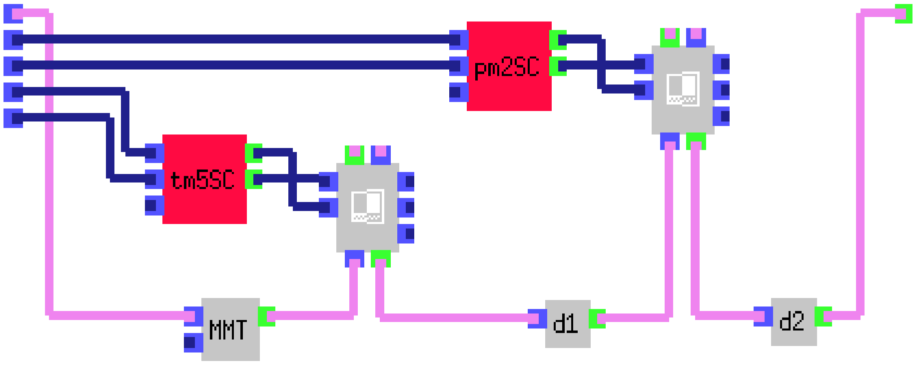

Table 4: **The ioMML module input/output ports.**

input	type	description
beam	field	input beam
PM_yaw	real	PM2 mirror yaw control signal
PM_pitch	real	PM2 mirror pitch control signal
TM_yaw	real	TM5 mirror yaw control signal
TM_pitch	real	TM5 mirror pitch control signal

output	type	description
out	field	output beam

Table 5: **Parameter settings for the ioMML primitive modules.**

name	primitive	parameter	settings	description
MMT	telescope	length lensinfo	1.24 (0.,0.6373),(1.065,0.6373)	total telescope length lens's parameters
PM2, TM5	mirror2	R L angle	0.9999 20.e-6 0.78539816	reflectivity loses turning angle
d1	propagator	have-delay length	no 2.102	non-delay propagator propagator length
d2	propagator	have-delay length	no 2.537	non-delay propagator propagator length

4.3 Mode Cleaner

Figure 5 shows the internal view of the ioMCC module. It has a mode cleaner module, the MC vertex mirror suspension controller (the $mcSC$ module) and one suspended turning mirror.

Figure 5: Block Diagram of the Mode Cleaner module.

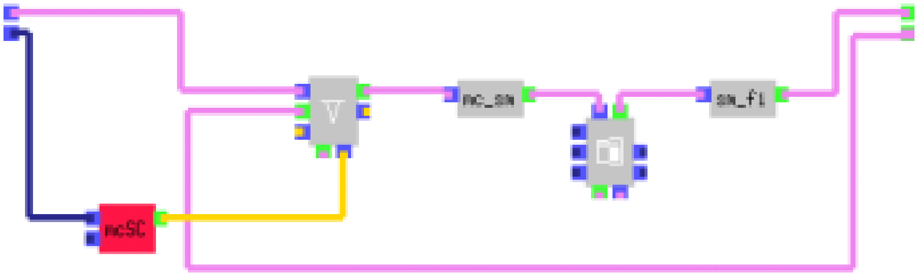

The Mode Cleaner is a triangular cavity for beam conditioning. Since it's very short (compare to the LIGO arm cavities) it is described as a summation module. In the End-to-End model there are two versions of the MC cavity primitive module: tri_mir_cav (standard), MC_cavity (customized). To calculate the cavity field the first module is using the Modal Model [6] and the second one is using the numerical FCD method [4]. We have checked this two modules against each other to get consistent results. The Mode Cleaner transfer function obtained in the simulation is shown in Figure 6. It corresponds to a simple low pass filter with pole at 3kHz.

One of the mode cleaner functions is to clean up the PSL beam suppressing the high order modes. Tables 6 shows the suppression factors for the first 10 Hermite-Gaussian modes calculated with the standard and customized MC cavities.

The MC vertex mirror suspension controller receives the MC length control signal from the LSC loop and send a correction signal to the vertex mirror taking into account the pendulum transfer

Figure 6: Mode Cleaner transfer function.

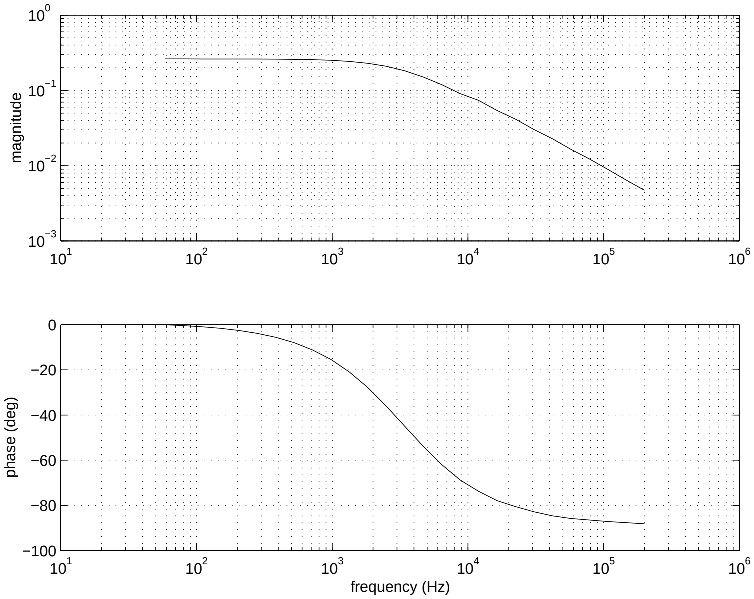

Table 6: **Transmission of the mode cleaner cavity for the first 10 Hermite-Gaussian modes.**

mode	00	01	01	02	11	20	03	12	21	30
units	%	ppm	ppm	ppm	ppm	ppm	ppm	ppm	ppm	ppm
tri_mir_cav	96.7	1.7	3.8	1.4	6.3	1.4	58	1.1	58	1.1

Figure 7: Internal view of the ioMMT module.

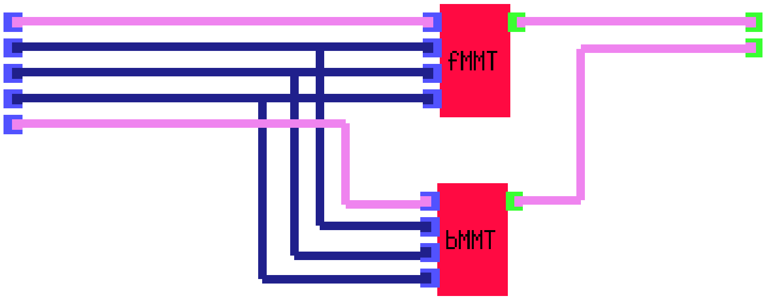

function.

4.4 IFO Mode-Matching Telescope

The Mode-Matching Telescope is used to optimize mode-matching of the IO beam into the IFO cavity. It has three suspended mirrors: MMT1, MMT2, MMT3. Only MMT3 mirror is controlled (mmtSC module). It receives the correction signals from the IFO ASC system (see Table 1). This optics is also used to transport the IFO reflected beam (the ifo_ref input port) back to the Faraday isolator where it is extracted to be sent into the IFO ASC (the FI_extr output port).

The ioMMT module internal structure is shown in Figures 7. It consists of two modules (fMMT, bMMT) with identical structure and the Faraday Isolator module that could be described as a thick lens. In the current simulation the FI module is trivial, thought we developed a thick lens primitive module that takes into account the thermo-lensing effect. The modules fMMT and bMMT have identical structure (Figure 8) and used to transport the main and reflected beams respectively.

5 Model of IO control systems

The Input Optics Control System consists of two subsystems:

1. Mode Cleaner Length and Frequency Control System (ioLSC)
2. Mode Cleaner Wave Front Sensing Control (ioWFS)

These two subsystems are shown on Fig.9.

5.1 MC Length Control System

This subsystem is used to lock the Mode Cleaner and maintain it in the lock. The control system is shown in Figure10 and can be described as follows.

Figure 8: Internal view of the fMMT (bMMT) module.

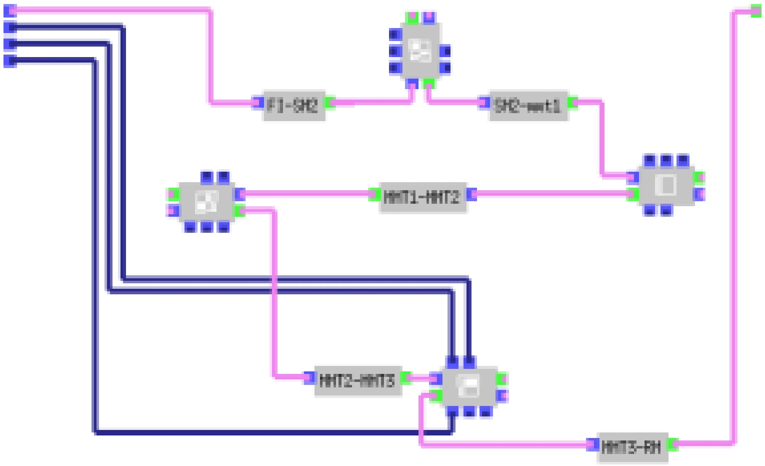

Figure 9: Block Diagram of the IO Control System.

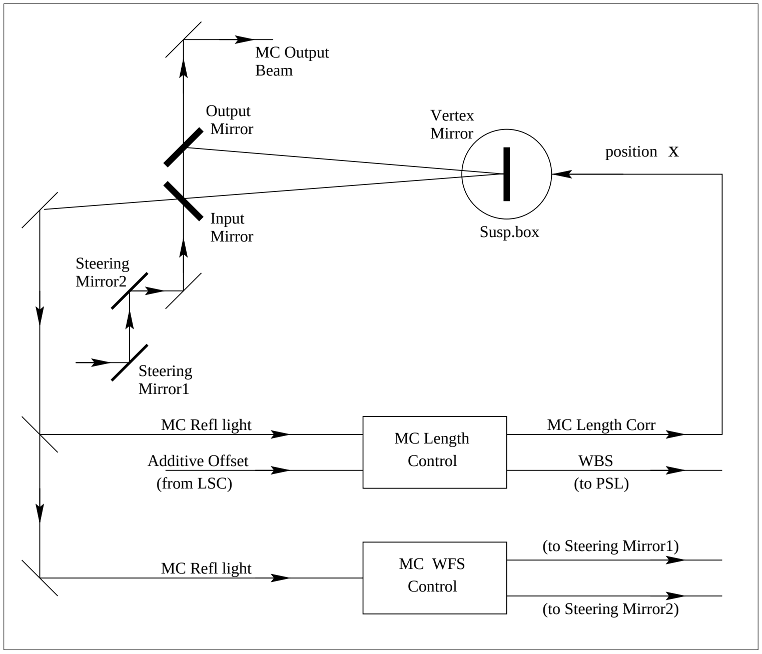

Table 7: **The ioLSC module input/output ports.**

input	type	description
MC_reflected	field	light reflected from the Mode Cleaner
k_mc_lock	real	MC lock sideband modulation frequency
offset	real	offset signal used by the LSC module
output	type	description
mc_length	real	correction signal for the MC end mirror
psl_wbs	real	PSL wide band signal

Figure 10: Block diagram of the ioLSC module.

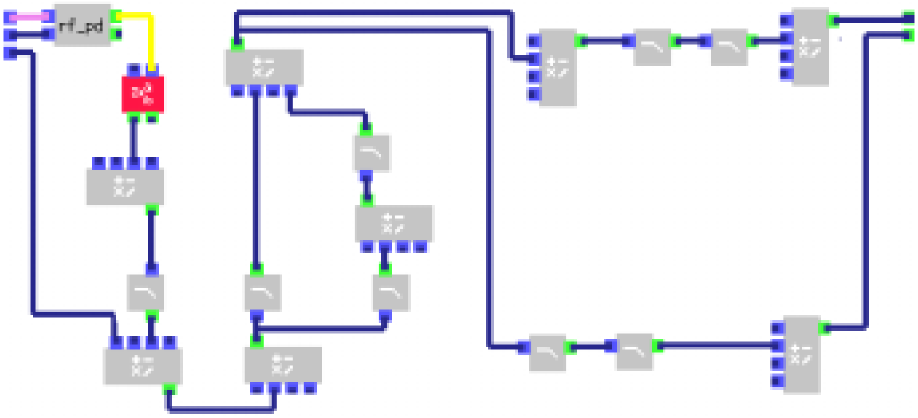

Mode Cleaner reflects the light to one of the view-ports. Part of the reflected light is the leakage light from inside of the Mode-Cleaner. This part carries information about the MC length. The reflected light is sent into the ioLSC module. A list of the module's input and output ports is shown in Table 7.

The internal view of the ioLSC module is shown in Figure 10. The MC reflected light is collected by the RF-tuned photo-diode (the $ioRFPD$ primitive module), which is a part of the Pound-Driver locking electronics. The output of the RF-tuned photo-diode is mixed with the signal from the local oscillator, which has the same frequency as the corresponding EOM (side-band generator) on the PSL table. The ioLSC module receives the modulation frequency from the ioEOM module through the input port k_mc_lock. The demodulated signal is sent to low frequency filters of the Length Sensing Control electronics. In the LSC electronics the signal is properly shaped by various filters that are implemented using the e2e digital filter primitive modules. For the filter's settings we used parameters from the LIGO note [7].

The ioLSC module has two outputs: mc_length and psl_wbs. The filtered output of the electronics, MC length error correction signal (the mc_length output port), is sent to the suspension controller (mcSC module) of the Mode-Cleaner vertex mirror. The open loop transfer function in the detection mode for this loop is shown in Figure **??**.

Figure 11: The open loop transfer function for feedback to the MC length.

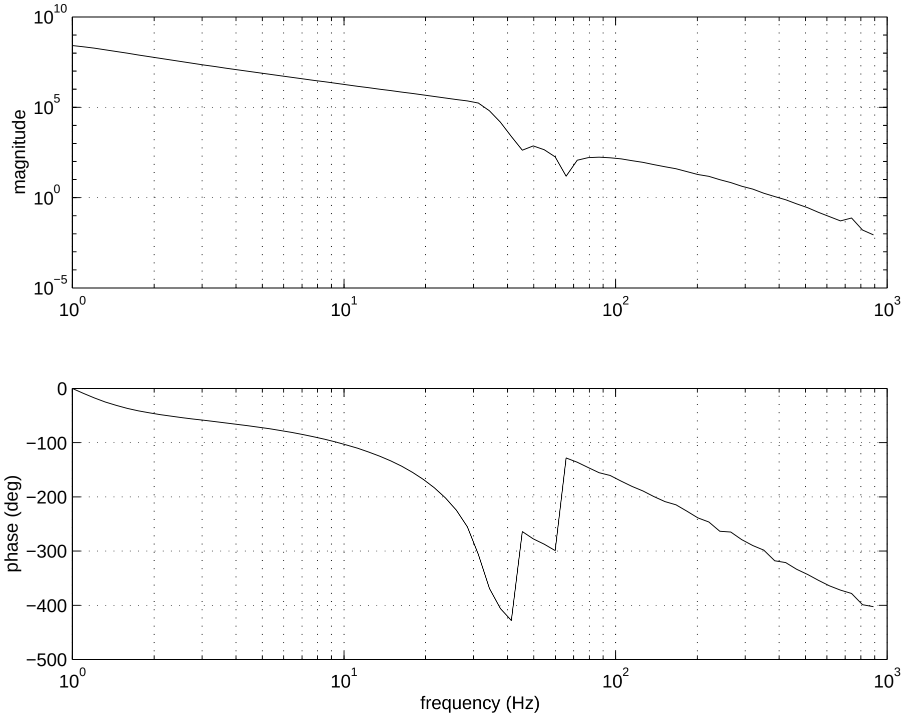

Another function of the MC Length/Frequency Control System is to correct the offset of the PSL laser Frequency Stabilization System (FSS). The ioLSC forms the Wide-Band Signal (psl_wbs output port), which is sent to the VCO (voltage-controlled oscillator) of the PSL. The open loop transfer function for the frequency control loop is shown in Figure 12.

5.2 MC Wave-Front Sensing Control

This servo maintains the pointing of the beam incident on the Mode Cleaner by controlling pitch and yaw angles of the two Steering Mirrors on the PSL table. The Wave-Front sensor operation is discussed in [9]. To implement the WFS simulation module we followed the note [8] where the design of the WFS Gouy phase telescope and photo-detectors can be found. The control loop block diagram is shown in Figure 15. Figure 16 shows the internal view of the Wavefront Sensing module (ioWFS). The ioWFS module takes the MC reflected beam and the WFS photo-diod demodulation frequency and returns the correction signals for steering mirrors pitch and yaw angles. The control loop is operating as described below: Reflected light from the Mode Cleaner is passed through the lens (the L_in module) to compensate for the divergence of the beam as it propagates a large distance (of order 4m) to the IOT-7 table.

At the IOT-7 table the beam is split by the beam splitter bsASC. Then the beams are expanded to match the surface of the Wave Front Sensor photo-diodes (WFS PD) by the lenses L_00 and L_90. This is necessary in to provide a right Gouy phase (180 degrees and 90 degrees respectively) on the

Figure 12: The open loop transfer function for the feedback to the PSL frequency.

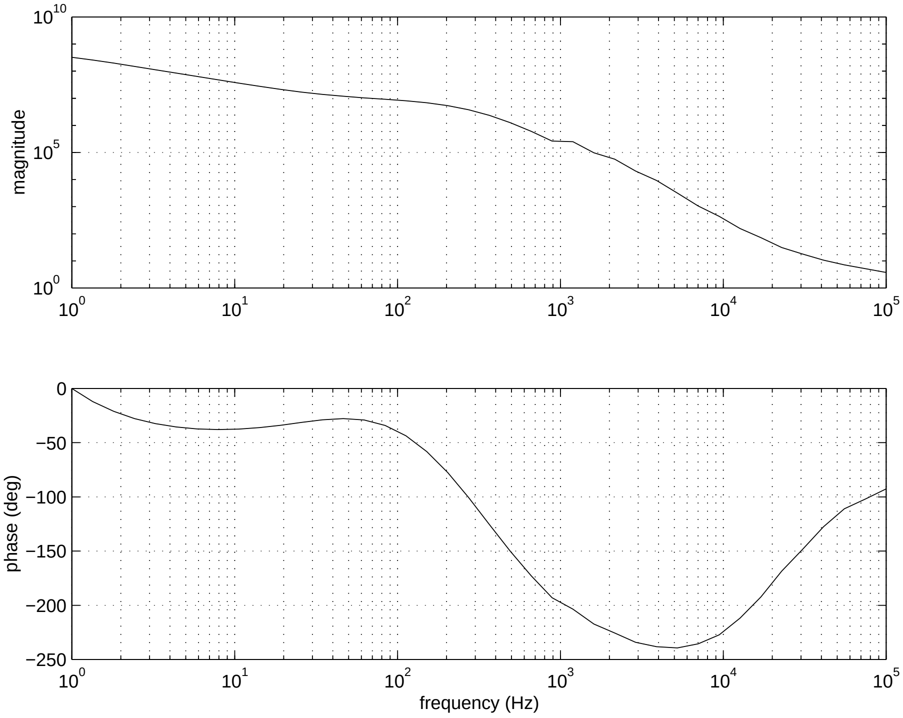

Figure 13: Block Diagram of the MC Demodulation Electronics

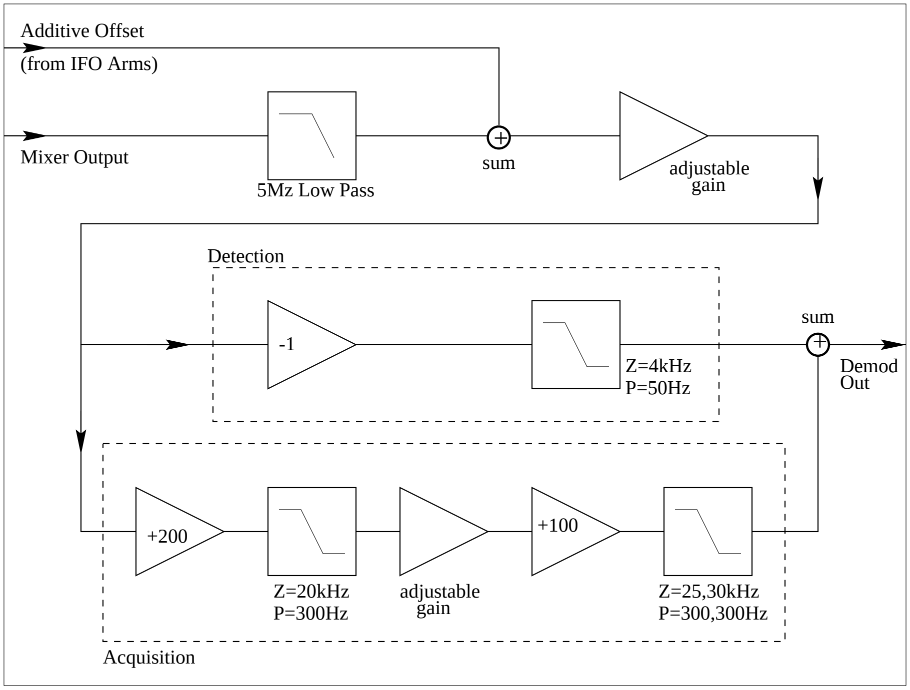

Figure 14: Block Diagram of MC Servo Amp

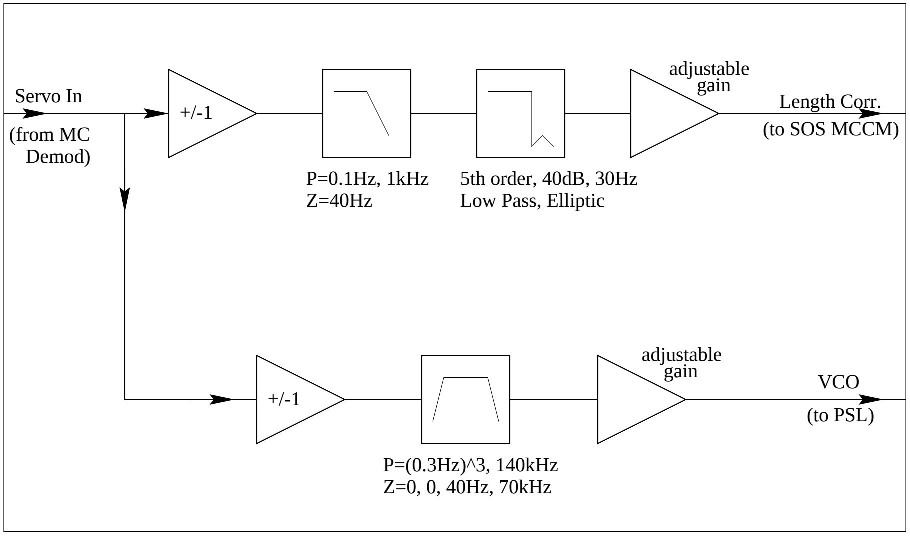

Figure 15: Block Diagram of the WFS and Steering Mirror Control

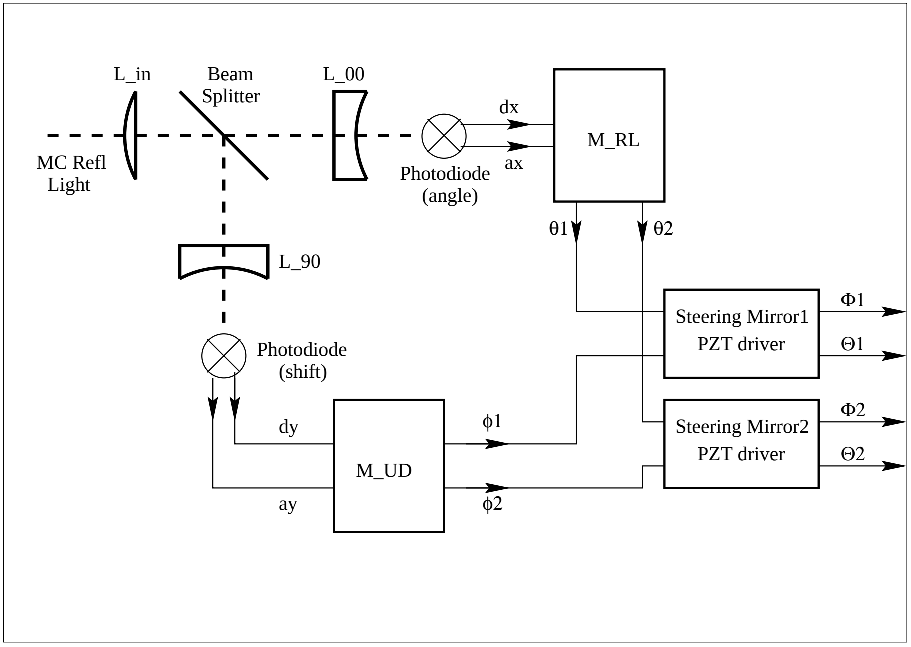

Figure 16: The internal view of the ioWFS module

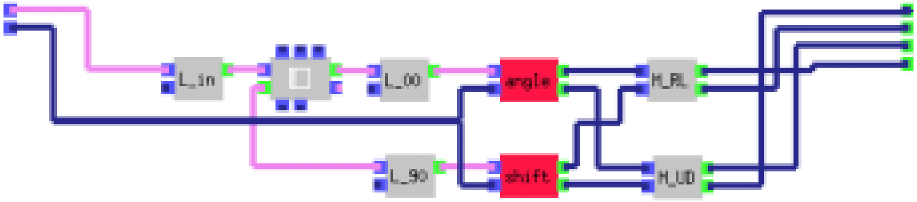

Figure 17: The internal view of the QPD module

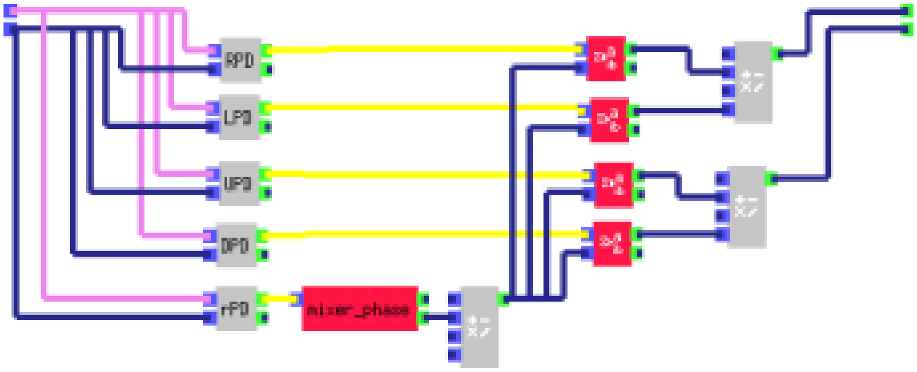

surface of the WFS PD.

Two signals formed by each photo-diode are proportional to the beam tilts (the $angle$ module) and the beam shifts ($shift$ module) on the input of the Mode Cleaner. The $angle$ and $shift$ modules have identical structure which is shown in Figure 17 (QPD.box configuration file). The input ports of the QPD module are: in - input field, $k - demod$ - the signal demodulation frequency.

A photo-diode which is used to detect alignment signals must be able to measure left/right and up/down asymmetry of the beam. In reality it is given by four-quad PD as shown in Figure **??**a. In the present simulation we used four primitive pd_demod modules (RPD, LPD,UPD, DPD) to describe each PD (Figure **??**b). The rPD module (reference PD) is used to apply a constant phase correction if one uses the input beam with arbitrary phase. The combination of pair of right-left (up-down) PDs forms the output alignment signal R_L (U_D) which are proportional to the beam tilts and shifts. To calculate the conversion constants from the sensor signals into the beam tilts and shifts we used a customized turning mirror module implemented using the FCD method [4]. It allows to tilt and shift input beam off the optical axis and calculate the mode composition of the output beam.

The output of the PD modules goes into the M_RL and M_UD modules that take into account the matrix which converts input beam tilts (Φ_x, Φ_y) and shifts (Δx, Δy) into steering mirrors yaw

$(\theta_{1x}, \theta_{2x})$ and pitch $(\theta_{1y}, \theta_{2y})$ angles:

$$\begin{bmatrix} \Delta x \\ \Phi_x \end{bmatrix} = \begin{bmatrix} 2d_1 & \sqrt{2}d_2 \\ 2 & \sqrt{2} \end{bmatrix} \begin{bmatrix} \theta_{1x} \\ \theta_{2x} \end{bmatrix}, \tag{1}$$

$$\begin{bmatrix} \Delta y \\ \Phi_y \end{bmatrix} = \begin{bmatrix} \sqrt{2}d_1 & 2d_2 \\ \sqrt{2} & 2 \end{bmatrix} \begin{bmatrix} \theta_{1y} \\ \theta_{2y} \end{bmatrix}, \tag{2}$$

where d1 (4.737 m) and d2 (2.632 m) are distances from the first (TM5) and second (PM2) mirrors respectively to the mode cleaner cavity waist. Note that the matrixes M_RL and M_UD are not identical because of the pitch/yaw asymmetry of a turning mirror. Since currently the End-to-End turning mirror can turn a beam only in one plane (horizontally), we modified the matrixes to accommodate this situation:

$$M\_RL = M\_UD = \begin{bmatrix} 2d_1 & \sqrt{2}d_2 \\ 2 & \sqrt{2} \end{bmatrix}. \tag{3}$$

Using the inverse matrixes $(M\_RL)^{-1}$ and $(M\_UD)^{-1}$ the matrix modules calculate the steering mirrors tilt angles. The output of the ioWFS module are sent to the ioMML module where it is handled by the Steering Mirror Control modules $tm5SC$ and $pm2SC$.

6 Usage of the IO simulation module.

The IO simulation module is a building block that can be used to describe any End-to-End configuration file. A simplest example of the configuration file is shown in Figure 18. It has a field source (laser), the IO module (ioo.box) and specified output ports. The configuration file can be created using the End-to-End Graphic User Interface Alfi [10]. The beam settings should correspond to nominal beam parameters on the input of the IO system: beam waist - 0.0005 m, waist position - 0.

Running the modeler (or modeler_freq) no time steps longer then $50\ \mu sec$ or shorter the MC round trip time ($0.102\ \mu sec$)can be used. If time step is longer then $50\ \mu sec$, the sommation approximation in the MC cavity is not valid and the MC transfer function begins to be different then one shown in Figure 6. If time step is shorter then the round trip time, the MC cavity built with the primitive modules should be used.

Figure 18: Example of the End-to-End configuration file test.box.

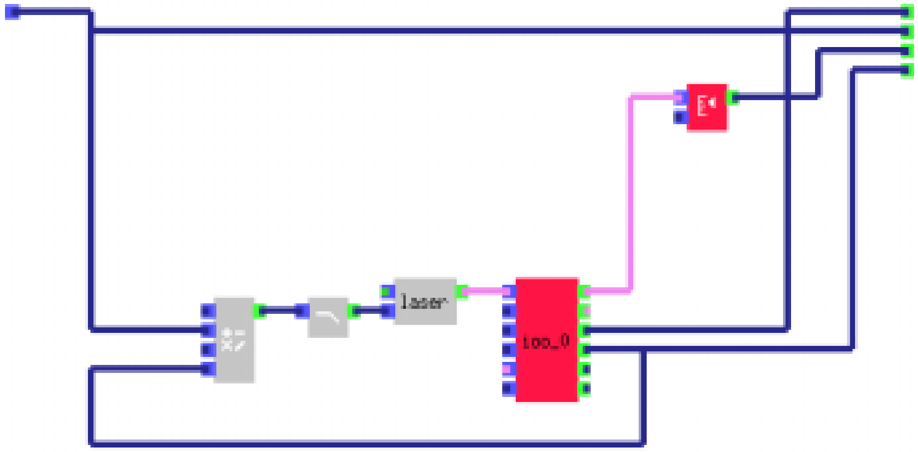

References

[1] B. Bhawal et al, LIGO-T970193-00-E, 1997 *Overview of the End-to-End model.*

[2] B. Bhawal et al, LIGO-T980051-00-E, 1998 *Getting started with End-to-End model.*

[3] B. Bhawal et al, LIGO-T990004-E, 1999 *Updates to the multi-mode version of the End-to-End model.*

[4] S.Klimenko, G.Mitselmakher LIGO-T990099-D, 1999 *Numerical Mode Decomposition.*

[5] R.Adhikari et al, LIGO-T980009-D, 1998 *Input Optics Final Design.*

[6] Y.Hefetz, N.Mavalvala, D.Sigg LIGO-T960005-R, 1996 *Principles of Calculating Alignment Signals in Complex Resonant Optical Interferometers.*

[7] P. Fritschel, N. Mavalvala, D. Ouimette. LIGO-T970218-02-D, 1997 *Mode Cleaner Length/Frequency Control Design.*

[8] D. Sigg, LIGO-T960111-A-D, 1996 *Wafefront Sensor.*

[9] N. Mavalvala, LIGO-T970098-01-D, 1997 *IO Mode Cleaner Wafefront Sensing and Control.*

[10] B. Bhawal et al, LIGO-T980014-01-E, 1998 *Alfi - GUI of the End-to-End Model.*